LOW-CYCLE FATIGUE BEHAVIOUR AND LIFETIME PREDICTION OF A SiC-PARTICULATE REINFORCED ALUMINIUM ALLOY AT ELEVATED TEMPERATURES

A. Jung, H. J. Maier, H.-J Christ*

ABSTRACT

The fatigue behaviour of a SiC-particulate reinforced dispersion-strengthened aluminium alloy was studied under fully reversed plastic strain-controlled conditions between room temperature and 300°C. Transmission electron microscopy revealed that cyclic stress-strain response is governed by the interaction between dislocations and the dispersoids, and quite similar microstructures were found to form independent of inelastic strain amplitude and test temperature. A multi-component model could thus be applied successfully to predict cyclic stress-strain behaviour.

Fatigue life was found to be reduced by the ceramic reinforcement as compared to an unreinforced reference material. As crack propagation governs fatigue life of both materials, lifetime at ambient temperature could be predicted quite accurately from crack growth data using the cyclic J-integral. At elevated temperature creep damage had to be taken into account and fatigue lives were predicted using the D_{CF} damage parameter instead. Extrapolation of data obtained to high-temperature long-term service conditions is discussed based upon the microstructural observations.

INTRODUCTION

Discontinuously reinforced aluminium-based metal-matrix composites possess attractive specific mechanical properties, and are thus promising candidate materials for various structural applications in the automotive and aerospace industries. Much work has been directed towards understanding the influence of the ceramic reinforcements on fatigue behaviour at ambient temperature. However, data on the high-temperature fatigue behaviour of these alloys is still rather limited. Recently aluminium alloys were developed that combine the microstructural stability of dispersoid-strengthened aluminium matrices with the low density and rather high elastic modulus of discontinuously reinforced alloys. The objective of the present study was to understand the effect of both the dispersoids and the ceramic reinforcement on cyclic stress-strain response and fatigue life at elevated temperatures. Hence, isothermal fatigue tests were performed on a SiC-reinforced dispersoid-strengthened aluminium alloy and its unreinforced counterpart.

MATERIALS AND EXPERIMENTAL DETAILS

The high temperature aluminium alloy X8019/SiC/12.5$_p$, which is reinforced with 12.5 vol.% SiC particles, and the unreinforced (i.e. SiC-free) reference alloy (8Fe-4Ce, in wt.%) were studied. Both alloys had been produced via a powder-metallurgy route and were supplied in the form of hot extruded bars. Iron, cerium and aluminium form fine, thermally stable intermetallic phases, which provide excellent microstructural stability of the matrix. Transmission electron microscopy (TEM) indicated that the microstructure of both alloys was almost identical regarding volume fraction, morphology of the dispersoids and grain size. Metallographic inspection of the as-received material revealed neither broken SiC particulates nor debonded SiC/matrix interfaces. The SiC particles, which had an average diameter of 2.8 μm, were found to be almost homogeneously distributed within the matrix. An average grain size of 1 μm was determined for both the reinforced and the unreinforced material. The temperature dependent monotonic tensile properties have already been reported earlier by Jung *et al.* (1).

For fatigue testing smooth cylindrical specimens with a gauge length of 16 mm and a gauge diameter of 7 mm were machined with the tensile axis parallel to the extrusion direction.

*Institut für Werkstofftechnik, Universität-GH Siegen, D-57068 Siegen, Fed. Rep. Germany

Prior to testing the gauge sections of the samples were polished mechanically with 1 μm diamond paste. All fatigue tests were run in air under symmetrical push-pull closed-loop inelastic strain control using a triangular function generator signal. The materials were tested at room temperature, 150°C and 300°C, respectively. The inelastic strain amplitudes ($\Delta\varepsilon_{in}/2$) applied were in the range from 0.025 to 0.4%. The magnitude of the inelastic strain rate $\dot{\varepsilon}_{in}$ was kept constant throughout the fatigue tests at a value of $1 \cdot 10^{-3}$ s^{-1} and $1 \cdot 10^{-5}$ s^{-1}, respectively.

Additional fatigue crack growth experiments on single edge notch bend specimens loaded in 4-point bending were conducted. These specimens were tested in the longitudinal-transverse orientation at a frequency of 50 and 170 Hz, respectively. The tests were performed at a constant stress ratio of $R = 0.1$ and 0.7, respectively.

Samples for scanning electron microscopy (SEM) studies were sectioned parallel to the external stress axis, polished and etched with Keller's reagent to reveal failure modes within the bulk material.

RESULTS

CYCLIC DEFORMATION BEHAVIOUR

The cyclic stress-strain response of both the SiC-reinforced and the unreinforced material was found to be very similar. After rapid initial hardening a pronounced region of cyclic saturation was observed. The unreinforced material showed a continuous drop in stress amplitude within the last ten percent of life due to macro crack propagation. In contrast, the reinforced material failed in a macroscopically brittle manner without a detectable change in the shape of the hysteresis loop. This behaviour was independent of the inelastic strain amplitude applied. Temperature affected only the magnitude of the stress amplitude.

Figure 1 shows the cyclic stress-strain (CSS) curve of the SiC-reinforced and the unreinforced material at different temperatures. A power-law describes the relationship between stress and inelastic strain at a given temperature reasonably well. As seen in Fig. 1 the difference in stress amplitude between the two materials diminishes at elevated temperatures. Furthermore, at low inelastic strain rates ($\dot{\varepsilon}_{in} = 1 \cdot 10^{-5}$ s^{-1}) the stress amplitude of the SiC-reinforced and the unreinforced alloy were found to be almost identical. This indicates that the strengthening role of the SiC particles diminishes with increasing temperature and decreasing inelastic strain rate.

FATIGUE LIFE

If compared based on strain amplitude, the addition of SiC particles decreased the fatigue life over the whole range of inelastic strain amplitudes applied. The fatigue life of both the SiC reinforced and the unreinforced material can be correlated with the inelastic strain amplitude according to the well known Coffin-Manson relationship. Figure 2 further demonstrates that temperature has only a minor influence on fatigue life. However, the damage mechanism was found to change drastically with temperature in the SiC-reinforced material. SEM examination of the fracture surfaces of samples fatigued at ambient temperature revealed numerous cracked SiC particles. The number of fractured particles increased with increasing length of the main crack. In contrast, metallographic studies of samples sectioned parallel to the stress axis revealed debonded particles but almost no cracked SiC particles in areas remote from the main crack. This indicates that fracture of the SiC particle occurs only in the stress field ahead of the main crack. The propensity for particle cracking also increased with particle size, because of the lower stresses required for cracking greater particles (Hall *et al.* (2)).

At elevated temperatures void formation at the SiC/matrix interface became dominant. Debonding of SiC particles and void formation at the poles of the SiC particles occured in fatigue tests run at 300°C. The SEM studies demonstrated that as the test temperature is increased fewer SiC particle are actually fractured. Thus, at high temperatures fatigue crack propagation within the matrix and/or void formation at the SiC/matrix interfaces govern fatigue life.

In contrast, few voids were found in the unreinforced alloy irrespective of test temperature. Both materials, however, were found to be similar with respect to crack initiation. Crack nucleation occurred always in near-surface regions, i.e. in the SiC-reinforced alloy cracks nucleated at large SiC particles and in the unreinforced material in iron-rich regions. Consequently, fatigue cracks formed rather easily within the first few cycles and crack nucleation does not contribute significantly to fatigue life.

MODELLING OF THE CYCLIC STRESS-STRAIN RESPONSE

For lifetime prediction using the fracture mechanics approach described later on, knowledge of the cyclic stress-strain response of the material is required. A multi-component model was used to predict the stress-strain path under various loading conditions at different temperatures. This model treats the material as a composite consisting of elastic-perfectly plastic elements with different yield stresses that are strained in parallel, for details see Christ (3). TEM observations revealed that subgrain formation played a significant role only in fatigue test run at 300°C and at the low inelastic strain rate of $1 \cdot 10^{-5}$ s^{-1}. For all other test conditions similar microstructures were observed, i.e. cyclic stress-strain response was found to be dominated by dislocation dispersoid interactions. Based upon these TEM observations the stress-strain response was modelled assuming a constant microstructure, i.e. a constant distribution of the local yield stresses of the individual elements irrespective of the actual test conditions. Test temperature and inelastic strain rate affect only the thermal component of the flow stress. For modelling, two hysteresis loops, one recorded at room temperature and another one monitored at 300°C, were used to first calculate the yield stresses of the individual elements and then the temperature dependence of the flow stress.
In Fig. 3a a hysteresis loop recorded in a test run at 150°C is compared to a calculated one. The excellent agreement between the measured and calculated stress-strain path is a direct consequence of the thermally stable dispersoids which govern the stress-strain response, i.e. basically the same microstructure prevails over the whole temperature range studied. Hence, the assumption that in fatigue tests at $\dot{\varepsilon}_{in} = 10^{-3}$ s^{-1} only the thermal component of the flow stress changes with temperature seems to be reasonable for the materials studied.

LIFETIME PREDICTION

As mentioned above, cracks are formed at an early stage of life. Thus, crack initiation is negligible and fatigue life can be predicted based upon crack growth only.
As proposed by Heitmann *et al.* (4), an approximation of the cyclic J-integral valid for semi-circular surface cracks under plain strain conditions was employed to characterize fatigue crack growth under fully plastified conditions. The fatigue life at room temperature can be determined by integrating the crack growth law

$$\frac{da}{dN} = B \cdot Z_D^m a^m . \tag{1}$$

B and m are constants that were obtained from crack growth measurements using single edge notch bend specimens. The parameter Z_D can be obtained directly from the hysteresis loop, for further details see (4). To predict fatigue life, knowledge of the initial crack length is essential. In the SiC-reinforced material initial crack length could be directly measured on the fracture surface in the SEM. An average value of 15 µm was obtained independent of the inelastic strain rate applied. Figure 4a demonstrates that fatigue life at ambient temperature of fully plastified samples can successfully be predicted based on crack growth data.
At temperatures above 250°C time dependent effects, i.e. creep, have to be taken into account. Riedel (5) introduced a damage parameter (D_{CF}) for creep-fatigue based on a material law for an elastic-viscoplastic solid:

$$D_{CF} = 1.45\frac{(\Delta\sigma_{eff})^2}{E} + 2.4 \cdot (1+3/n)^{-1/2} \Delta\sigma\Delta\varepsilon_{pl}\left[1+\left(\frac{\Delta\varepsilon_{cr}}{\Delta\varepsilon_{pl}}\right)^{1+n'}\right], \tag{2}$$

where $\Delta\varepsilon_{in} = \Delta\varepsilon_{pl} + \Delta\varepsilon_{cr}$. The Norton exponent n was obtained from creep experiments and the fatigue hardening exponent n' was calculated from the slope of the CSS curve (c.f. Fig. 1). The other quantities were determined solely by analysing a hysteresis loop recorded in cyclic saturation. The effective stress range can be calculated as a function of stress ratio R (4) as

$$\Delta\sigma_{eff} = \Delta\sigma \cdot 3.72 \cdot (3 - R)^{-1.74} \tag{3}$$

It should be noted that for time-independent crack growth, i. e. for $\Delta\varepsilon_{cr} = 0$, the damage parameters D_{CF} and Z_D are equivalent.

In the original analysis slow-fast tests and experiments with hold times were used to calculate D_{CF}. In such tests the amount of creep strain $\Delta\varepsilon_{cr}$ is determined rather easily. In the present study special fatigue tests were devised to determine the contribution of creep deformation to the inelastic strain at high temperatures. In these tests samples were cycled initially at $\Delta\varepsilon_{in}/2 = 0.4\%$ and a rather low inelastic strain rate of $\dot{\varepsilon}_{in} = 1 \cdot 10^{-5}$ and $1 \cdot 10^{-3}$ s^{-1}, respectively. Once cyclic saturation was established, the inelastic strain rate was changed instantaneously to $\dot{\varepsilon}_{in} = 1 \cdot 10^{-2}$ s^{-1} at the minimum strain. Figure 3b shows the hysteresis loops obtained in such a test. As microstructure does not vary rapidly, both hysteresis loops are recorded without any significant microstructural change. Additional tests clearly demonstrated that at $\dot{\varepsilon}_{in} = 1 \cdot 10^{-2}$ s^{-1} the contribution of creep to inelastic strain is negligible. Hence, the plastic strain and the creep strain component of inelastic strain can be obtained approximately by comparing the two hysteresis loops as shown in Fig. 3b. Then, fatigue life can be calculated by integrating the crack growth law in Eq. 1, but replacing Z_D with D_{CF}. The coefficients B and m were again taken from fatigue crack growth measurements. Note that data obtained on the unreinforced material at ambient temperature were used, as the SEM studies had indicated that high-temperature fatigue is governed by void formation and fatigue crack growth in the matrix. The predicted and the measured fatigue lives for the reinforced alloy at 300°C are compared in Fig. 4b.

DISCUSSION

As revealed by TEM, deformation behaviour is governed mainly by the interaction between dislocations and dispersoids. Still, at ambient temperature high localized inelastic strains develop as a result from the constraint on the matrix from adjacent SiC particles (Llorca *et al.* (6)). Thus, the stress amplitude is different for any given inelastic strain amplitude in the SiC-reinforced alloy as compared to the unreinforced material, c.f. Fig. 1. At elevated temperatures strain localization is less significant, and the overall cyclic stress-strain response of the SiC-reinforced alloy becomes quite similar to that of the unreinforced material at 300°C. Similarly, Vyletel *et al.* (7) reported only small differences in dislocation arrangement and cyclic stress response between a TiC-reinforced artificially aged aluminium alloy and its unreinforced counterpart as long as the precipitates were not sheared.

Whereas the SiC-reinforcement had only a small effect on stress-strain response, fatigue life was found to be significantly different for both alloys studied. At ambient temperature, extensive damage is accumulated as result of the highly localized inelastic strains adjacent to the SiC particles. Furthermore, finite-element analysis revealed that the inhomogeneous distributions of stresses and strains induced by stiff particles are enhanced at a free surface relative to the interior of the material (Levin and Karlsson (8)). Thus, cracks are formed rather easily at SiC particles within the first few cycles as observed in the present study. As fatigue life is dominated by crack growth, the cyclic J-integral was found to be an appropriate damage parameter to predict fatigue life under fully plastified loading conditions. In the unreinforced material rapid crack initiation occurred at iron-rich near-surface defects, and the cyclic J-integral approach can thus be used for the unreinforced material as well. However, initial crack length is different in both materials. As many cycles are spent in early crack growth, part of the degradation in fatigue life caused by the SiC reinforcement, c.f. Fig. 2, directly results from the difference in initial crack length.

At elevated temperatures above about 250°C voids are formed at the SiC/matrix interfaces and creep damage contributes significantly to fatigue life. Under such conditions D_{CF} becomes an appropriate damage parameter. Due to the microstructural stability of the dispersoids up to temperatures of 450°C (Yaney and Nix (9)) a moderate extrapolation of cyclic deformation behaviour to higher temperatures and/or extended time periods appears to be reasonable. Similarly, the correlation between the D_{CF} parameter and the numbers of cycles to failure given in Fig. 4b can be used to predict lifetime as long as the damage mechanisms does not change. In high-temperature slow strain rate ($\dot{\varepsilon}_{in} = 1 \cdot 10^{-5}$ s^{-1}) tests, damage can be controlled by the coalescence of voids and lifetime can no longer accurately be predicted by integrating the crack growth rate based upon the D_{CF} damage parameter (Renner *et al.* (10)). Creep damage is less pronounced in the unreinforced material where grain and subgrain boundary are pinned by the dispersoids. Hence, grain boundary migration is restricted as is void formation at grain boundaries, and it is assumed that the D_{CF} parameter can be used to predict lifetime under conditions were it will no longer hold for the SiC-reinforced material.

Acknowledgement-Financial support of this study by Deutsche Forschungsgemeinschaft is gratefully acknowledged.

REFERENCES

(1) Jung, A., Maier, H.J. and Christ, H.-J., Proc. of 5th Europ. Conf. on Advanced Materials, Processes and Applications, Euromat '97. Edited by L.A.J.L. Sarton, H.B. Zeedijk, Zwijndrecht, 1997, pp. 1/277-1/282.
(2) Hall, J.N., Jones, J.W. and Sachdev, A.K., 5th Int. Conf. on Fatigue and Fatigue Thresholds, FATIGUE '93. Edited by J.-P. Bailon, J.I. Dickson, Montreal, 1993, pp. 1129-1135.
(3) Christ, H.-J., „Wechselverformung von Metallen". Edited by B. Ilschner, Springer, Berlin, 1991.
(4) Heitmann, H.H., Vehoff, H. and Neumann, P., „Advance in Fracture Research 84", Proceedings of ICF 6. Edited by S.R. Valluri, Pergamon Press, Oxford, 1984, pp. 3599-3606.
(5) Riedel, H., „Fracture at High Temperatures", Materials Research and Engineering. Edited by B. Ilschner and N.J. Grant, Springer, Berlin, 1987.
(6) Llorca, J., Suresh, S. and Needleman, A., Met. Trans., Vol. 23A, 1992, pp. 919-934.
(7) Vyletel, G.M., Allison, J.E. and Van Aken, D.C., Met. Trans., Vol. 24A, 1993, pp. 2545-2557.
(8) Levin, M., Karlsson, B., Int. J. Fatigue, Vol. 15, 1993, pp. 377-387.
(9) Yaney, D.L., Nix, W.D., Met. Trans., Vol. 18A, 1987, pp. 893-902.
(10) Renner, E., Vehoff, H. and Neumann, P., Fatigue Fract. Engng. Mater. Struct., Vol. 12, 1989, pp. 569-584.

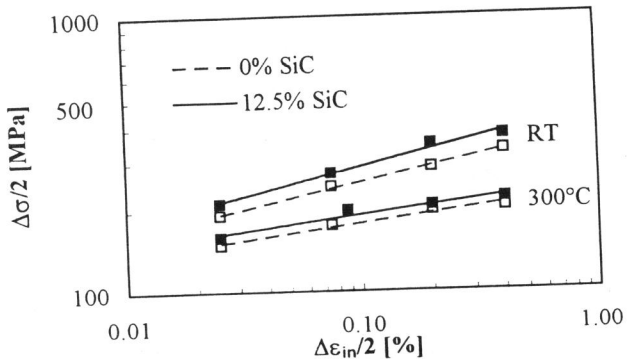

Fig. 1. Cyclic stress-strain curves of the SiC-reinforced and the unreinforced material at different temperatures.

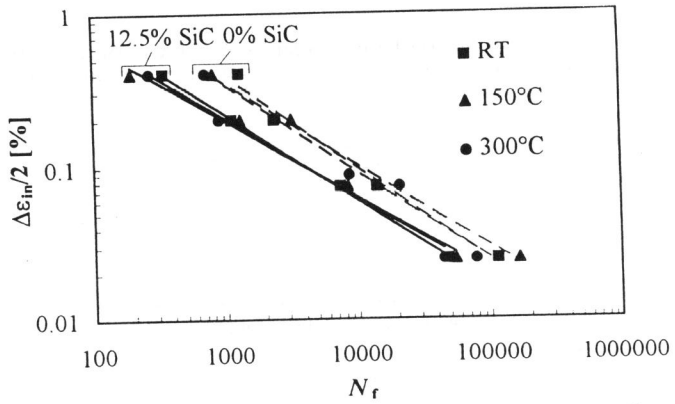

Fig. 2. Coffin-Manson plot for the SiC-reinforced and the unreinforced alloy at different temperatures and $\dot{\varepsilon}_{in} = 10^{-3}\ s^{-1}$.

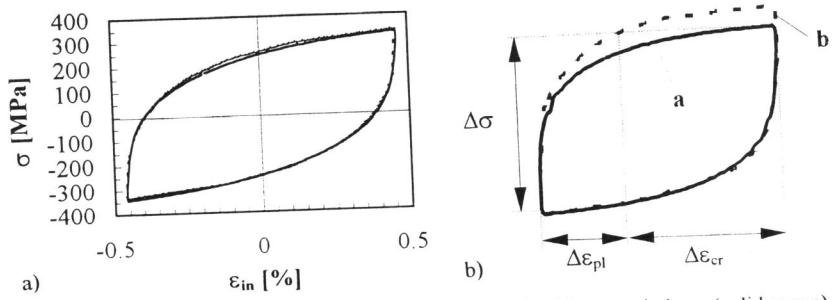

Fig. 3. (a) Comparison between an experimentally obtained hysteresis loop (solid curve) of the SiC-reinforced alloy and a predicted one (dashed curve) at T = 150°C, $\Delta\varepsilon_{in}/2$ = 0.4% and $\varepsilon_{in} = 10^{-3}\ s^{-1}$; (b) two hysteresis loops measured at 300°C in the cyclic saturation state. Please note that hysteresis loop **a** ($\varepsilon_{in} = 1 \cdot 10^{-3}\ s^{-1}$) and **b** ($\varepsilon_{in} = 1 \cdot 10^{-2}\ s^{-1}$) are shifted to their compressive load reversal points.

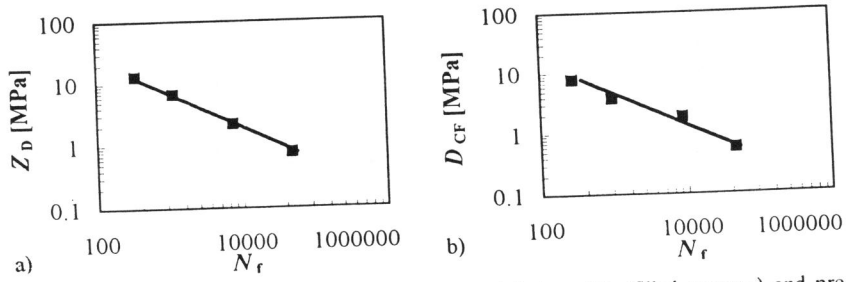

Fig. 4. Comparison between experimentally obtained fatigue life (filled squares) and predicted lifetime of the SiC-reinforced alloy at (a) room temperature (b) 300°C. See text for details.